

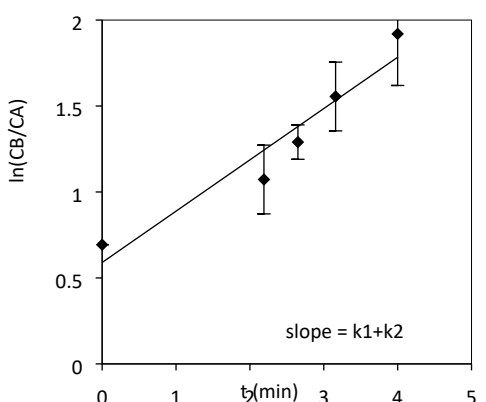
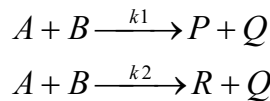
Assessment of multipoint dosing approach for Exothermic Nitration in CSTRs in series

G. M. Mule,^{a,b} S. Kulkarni^b and A. A. Kulkarni^{a,b}

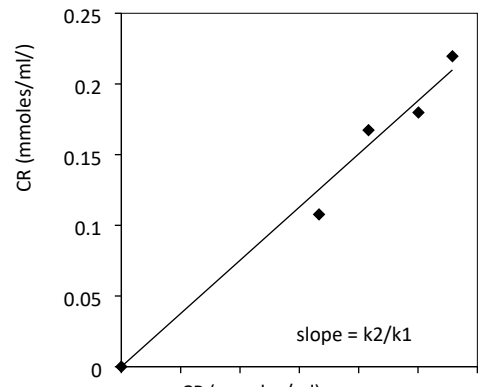
Supporting Information

S1: Kinetic study from the raw data

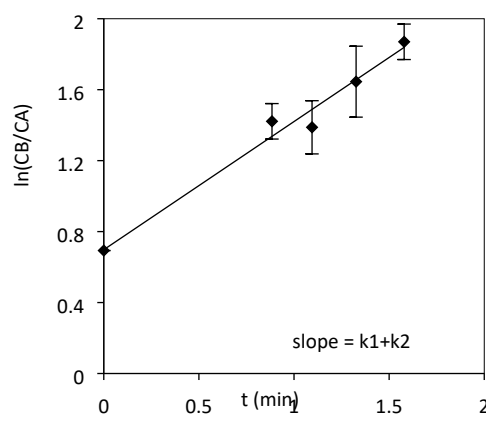
As mentioned in the main article, separate experiments were carried out to determine the rate constants of the reaction at different temperatures. Given below the plots of conversion with respect to time at different residence time.



A



B



C

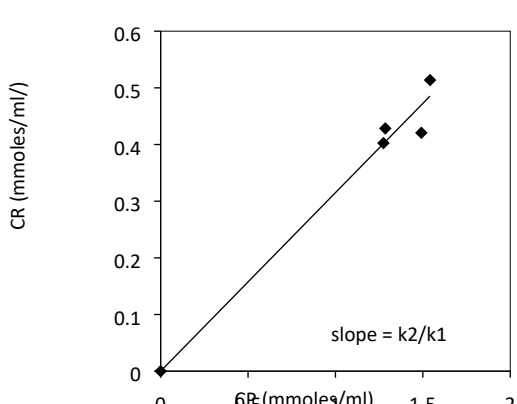


Figure S1: A) Concentration vs time at 40 °C, B) Moles of R (isomer) produced vs moles of P (product) produced at 40 °C, C) Concentration vs time at 60 °C, D) Moles of R (isomer) produced vs moles of P (product) produced at 60 °C

The data was fitted against the second order bimolecular reaction kinetics and fit was accurate.¹ Figure S1 shows that increase in reaction temperature leads to higher reaction rates as well as isomer ratio (undesired to desired). With two sets of equation obtained from the experimental data, k_1 and k_2 can be calculated for said reaction temperature and exercise can be repeated for different temperatures. Once rate constants are obtained with respect to temperature, activation energy and pre-exponential factors can be calculated, which makes rate of reaction a function of temperature and initial concentrations of reagents. The values of activation energy and pre-exponential factor is provided in the main article.

S2: Effect of various parameters on the production

S2.1 Initial concentration (C_{A0}) and molar flow rate ratio (F_{B0}/F_{A0})

Keeping the volume of the reactor as same as experimental the effect of initial concentration of A (C_{A0}) and molar flow ratio was studied using numerical simulations. Figure S2(A-C) illustrates the effect on the temperature. From the figures, it can be observed that for a fixed initial concentration of A , the temperature in the reactor goes down with an increase in F_{B0}/F_{A0} . Similar observations can be made by low initial concentration at fixed F_{B0}/F_{A0} . This is entirely attributed to the dilution in the system. With constant residence time and volume of the reactor, the total volumetric flow rate gets fixed. Therefore, at higher F_{B0}/F_{A0} the concentration of A in the well-mixed reactor is much lesser compared that at lower F_{B0}/F_{A0} . However, the conversion at higher F_{B0}/F_{A0} is higher compared to that at lower F_{B0}/F_{A0} , which

almost attains plateau after $\frac{F_{B0}}{F_{A0}} = 2$ (see Figure S2(E)). In addition, the production is fairly high

at $\frac{F_{B0}}{F_{A0}} = 2$ (see Figure S2(F)). These studies reveal that $\frac{F_{B0}}{F_{A0}} = 2$ with $C_{A0} = 5.7$ milimoles/ml are the optimized operating conditions for CSTRs.

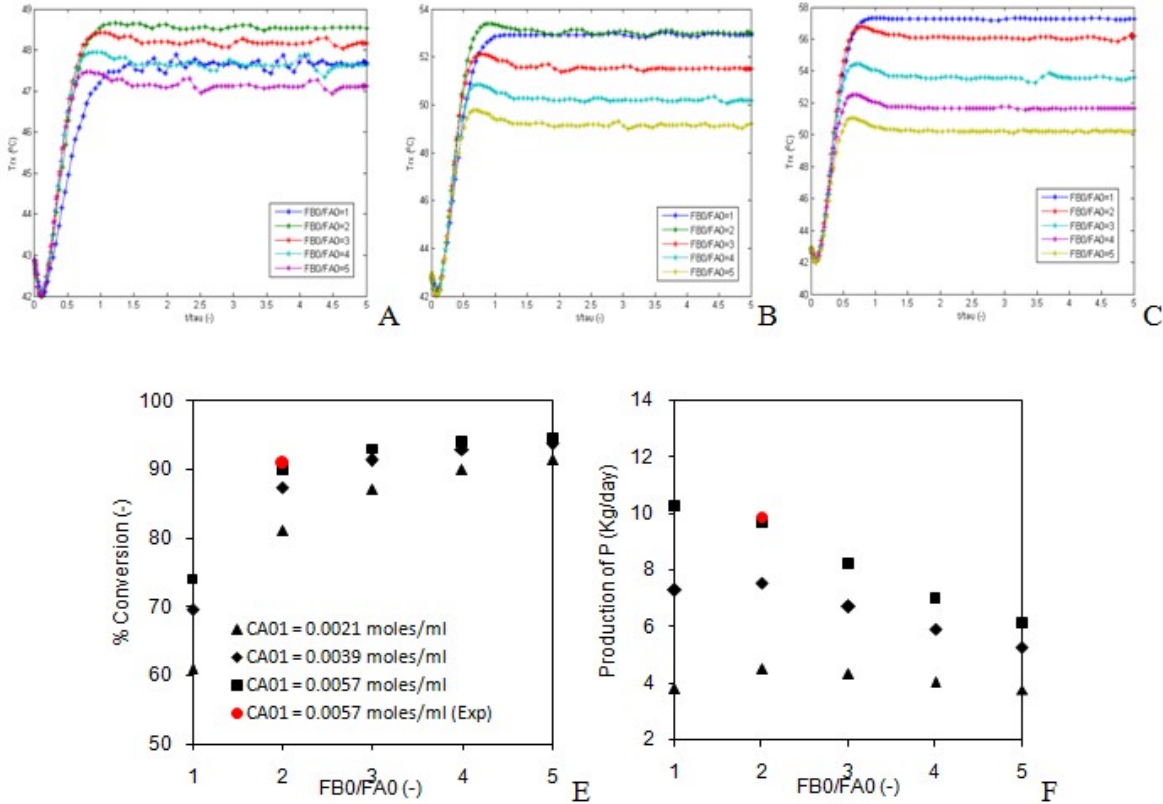


Figure S2. Reactor temperature profiles at different molar ratio A) $C_{A0}=2.1$ milimoles/ml, B) $C_{A0}=3.9$ milimoles/ml, C) $C_{A0}=5.7$ milimoles/ml, E) Conversion vs Molar flow ratio (F_{B0}/F_{A0}), F) Production (kg/day) vs Molar flow ratio (F_{B0}/F_{A0}).

In general, production of the desired product depends on several parameters such as residence time (τ), volume of the reactor (V), temperature of the reactor (T_{rx}), molar flow ratio of the reactants (F_{B0}/F_{A0}), initial concentration of the reactants (C_{A0}, C_{B0}) and coolant temperature ($T_{J_{in}}$). It becomes important to study the effect of these parameters to come up with better-operating conditions. Simulations for various such parameters were carried out to come up with the scale-up strategies.

S2.2 Effect of volume of the reactor (V) and Residence time (τ)

Results from the last section were taken into consideration for studying the effect of volume of the reactor (V) and the residence time (τ). The initial concentration of A (C_{A0}) was maintained at 5.7 milimoles/ml and molar flow rate ratio (F_{B0}/F_{A0}) as 2. The calculations were done considering glass jacketed reactors where jacket inlet ($T_{J_{in}}$) temperature was set at 27 °C. It

should be noted that all the scale up guidelines were followed and scale up related equations are given in Appendix 1. Figure S3(A-B) shows that the CSTR can be operated at higher residence time and at a larger volume of the reactor, as the temperature in the reactor for this range is 60 ± 10 °C. Also, the percent conversion of reactant ‘A’ is on the higher side. However, the production at this range of τ and V is the minimum. Therefore, by considering all the three requirements (T_{rx} , conversion and highest production), the acceptable operating point would change in terms of the reactor volume and the residence time.

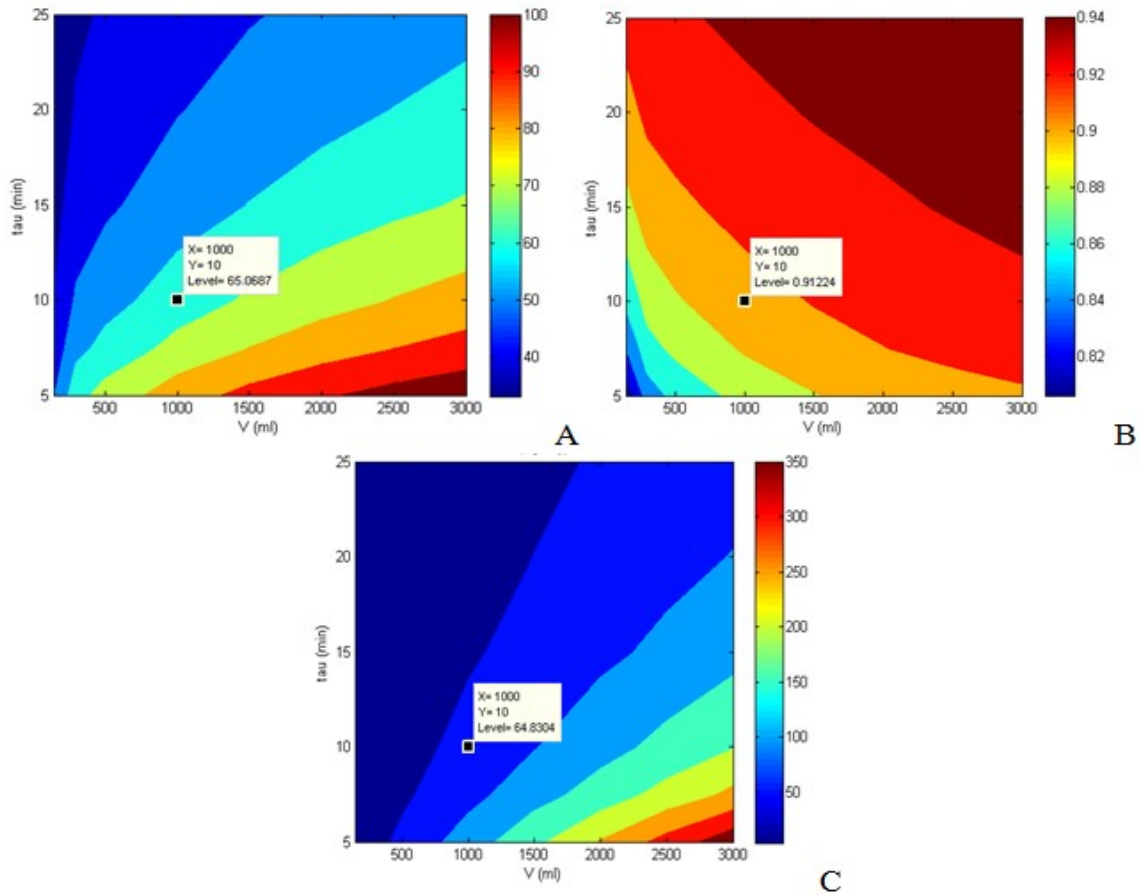


Figure S3: Effect of volume of the reactor and residence time on A) Temperature (T_{rx}) in the reactor (X (Volume, ml) = 1000, Y (τ) = 10, Level (T_{rx}) = 65.05 °C), B) Percent conversion X (Volume, ml) = 1000, Y (τ) = 10, Level (Conversion) = 0.91), C) Production (kg/day) X (Volume, ml) = 1000, Y (τ) = 10, Level (Production)= 64.83 Kg/day).

S2.3 Effect of coolant inlet temperature (T_{Jin}) and coolant mass flow rate (m_c)

The effect of T_{Jin} and m_c on the steady state operation was studied using the energy balance equation. The steady state point of CSTR operation is said to be achieved when heat-generated curve intersects with that of heat-removal (see Figure S3). The equations equation for both the curves are given below¹;

$$Q_R = m_c C_{Pc} (T_{rx} - T_{Jin}) \left(1 - \exp \left(\frac{-UA}{m_c C_{Pc}} \right) \right) + F_{A0} \sum \phi_i C_{Pi} (T_{rx} - T_A) \quad (1)$$

$$Q_G = (r_A) V (-\Delta H_{Rx}) = -F_{A0} X_A (-\Delta H_{Rx}) \quad (2)$$

here, Q_R and Q_G are heat removal and heat generation curves respectively. The heat generation curve is plotted against the temperature using mole balance. However, the heat removal curve is plotted against the temperature using flow and heat exchange. A careful observation of Figure S4(A), suggest that one would observe more than one steady state if parameters changed slightly. However, the operation conditions for such scenario is ruled out in the present study as to minimize the operating cost by feeding coolant above 15 °C. In this case only a single intersection point between Q_R and Q_G can be observed (Figure S4(B)). Hence the effect of coolant inlet temperature and coolant flow rate on steady state operation was studied. From Figure S4, it can be observed that the increase in the coolant inlet temperature shifts the steady state towards unsafe operation. On the other hand, increase in the coolant flow rate more than 5 ltr/min does not result in much change in the operating conditions (see Figure S4(C)). This

is attributed to the term $\exp \left(\frac{-UA}{m_c C_{Pc}} \right)$ in the energy balance equation.

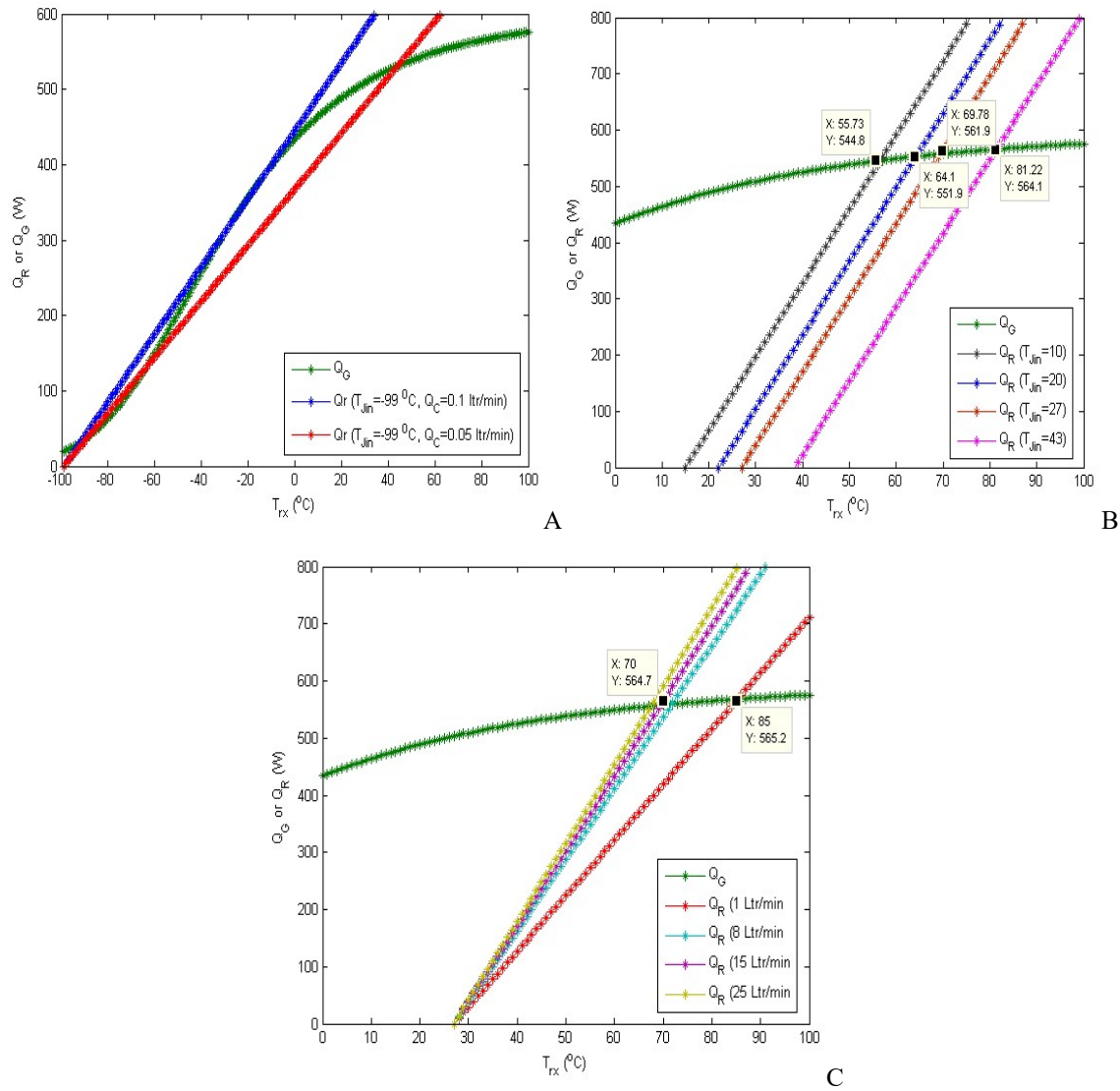


Figure S4: Effect of coolant parameters A) Multiple steady states, B) Coolant inlet temperature, C) Coolant flow rate

S3: Scale-up Strategies

Safety concerns are more noticeable in the large volume CSTRs to meet the desired production per day. Therefore, it is essential to discuss various strategies related to scale up of CSTRs. For the conviction, it was decided of the setting of a plant of minimum 150 Kg/day of Nitro-naphthalene. It should be noted that the feasible operating range should be between 45 °C to 70 °C to avoid un-necessary events related to safety, as discussed above. Temperature in the reactor depends on the various parameters such as T_{Jin} , operating volume (V), initial concentration of Naphthalene (C_{A0}), residence time (τ) molar flow rate ratio (F_{B0}/F_{A0}) and material of construction of the vessel. As per the scale up guidelines, the residence time and molar flow rate ratio has been maintained as that of lab scale (experimental). The effect of all these parameters was studied to come up with best scale-up strategies. To minimize the

operating cost, simulations for scale-up strategies were carried out for $T_{jin}= 27$ °C. All the results are compiled and discussed in the later part of the section.

S3.1 Scheme I: Glass reactors configuration

Initially, conversion and operating temperature at different reactor volume and residence were simulated and studied (see Figure S5). For a residence time of X minutes for operating volume less than $100X$ ml, scale-up is feasible and it can produce only $7X$ Kg/day of the desired mono-nitro derivative (Figure S4(B)) and any further increase in the volume can only increase the reactor temperature exponentially along with incomplete conversion (Figure S5(C)).

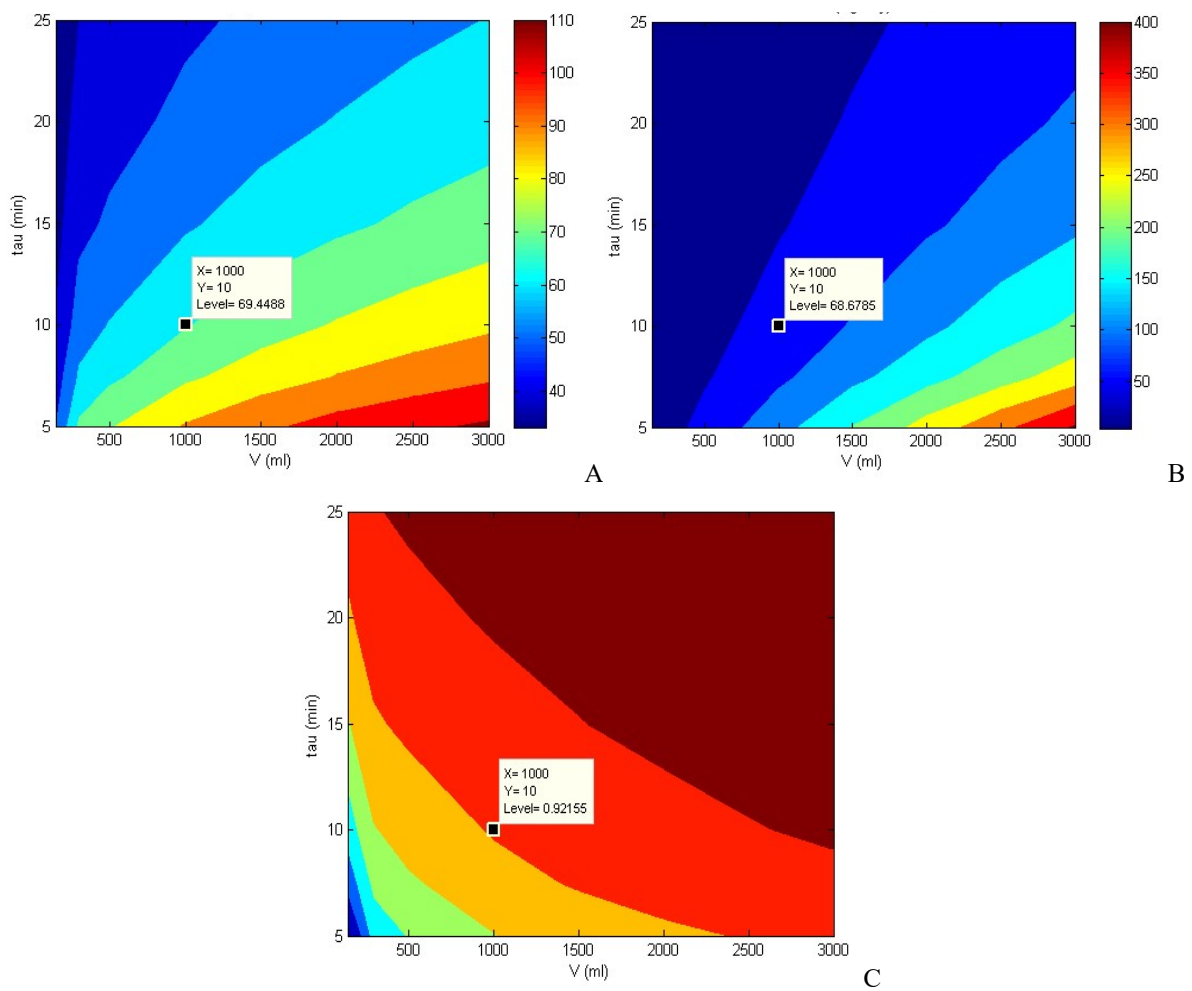


Figure S5: Effect of residence time and operating volume on various parameters for glass reactors A) Temperature in the reactor, B) Production, C) Conversion.

Conventionally, it is known that the required production can be achieved by using more number of identical volume reactors in parallel, while close to complete conversion can be achieved by carrying out an operation in series of CSTRs. Keeping in mind the feasibility of operation, using parallel CSTRs (say n number) of $100X$ ml each followed by a CSTR of $100.n.X$ ml found to be the best choice for achieving the production of $75.n.X$ Kg/day. The temperature profiles of the reactors are given in the Figure S6 with multiple reactors in parallel followed by a large reactor in series. The conversion and yield at the outlet of the reactor can be optimized to 98% and 92%, respectively. The production of the desired product can be achieved as close to $7.5n.X$ Kg/day within the temperature limits of 45°C to 70°C .

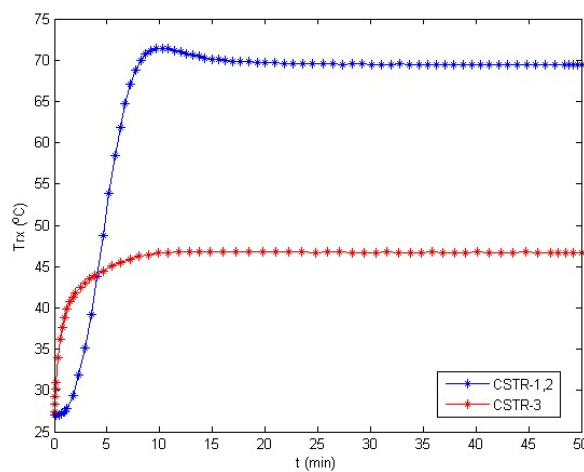


Figure S6: Temperature in the reactors in parallel and in series

S3.2 Scheme II: SS316 reactors configuration

Similar to the glass reactors, initially study for single CSTR of different volume at different residence time was carried out. And the results showed that SS316L reactor volume up to $300X$ ml can be used. The simulations showed that single CSTR made up of SS316L can produce up to $20X$ Kg/day however it achieves the conversion of 90% and hence an additional CSTR in series can help in achieving the nearly complete conversion. The temperature profile in such reactors in series is presented in Figure S7.

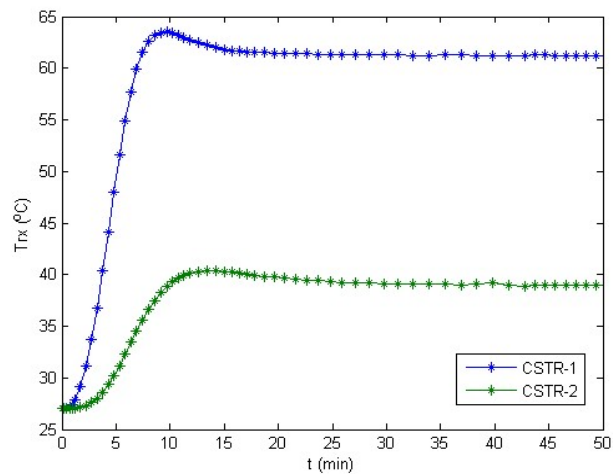


Figure S7: Temperature in the reactors

References

1. Fogler, H. S., Elements of chemical reaction engineering. **1999**.
2. Levenspiel, O., Chemical reaction engineering, John Wiley and sons, **1998**.